remote sensing

MDPI

Article

Spectral Angle Mapper Application Using Sentinel-2 in Coastal Placer Deposits in Vigo Estuary, Northwest Spain

Wai L. Ng-Cutipa [1,2,*], Ana Lobato [1], Francisco Javier González [1], Georgios P. Georgalas [3], Irene Zananiri [3], Morgana Carvalho [4], Joana Cardoso-Fernandes [4], Luis Somoza [1], Rubén Piña [2], Rosario Lunar [2] and Ana Claudia Teodoro [4]

[1] Marine Geology Resources and Extreme Environments, Geological Survey of Spain (IGME-CSIC), Calle Ríos Rosas 23, 28003 Madrid, Spain; ab.lobato@igme.es (A.L.); fj.gonzalez@igme.es (F.J.G.); l.somoza@igme.es (L.S.)
[2] Departamento de Mineralogía y Petrología, Facultad de Ciencias Geológicas, Universidad Complutense de Madrid, Calle Jose Antonio Novais 12, Ciudad Universitaria, 28040 Madrid, Spain; rpinagar@geo.ucm.es (R.P.); lunar@ucm.es (R.L.)
[3] Hellenic Survey of Geology & Mineral Exploration (HSGME), Spirou Loui 1, 13677 Athens, Greece; ggeorgalas@eagme.gr (G.P.G.); izananiri@eagme.gr (I.Z.)
[4] Institute of Earth Sciences, Faculty of Sciences, University of Porto, Rua Campo Alegre s/n, 4169-007 Porto, Portugal; morgana.carvalho@fc.up.pt (M.C.); joana.fernandes@fc.up.pt (J.C.-F.); amteodor@fc.up.pt (A.C.T.)
* Correspondence: wl.ngcutipa@igme.es

Abstract: Remote sensing applications for marine placer deposit exploration remain limited due to the mineralogical complexity and dynamic coastal processes. This study presents the first medium- to high-level detailed multi-scale remote sensing analysis of placer deposits in the Rías Baixas, NW Spain, focusing on five beaches within the Vigo Estuary. Ten beach samples were analyzed for their heavy mineral (HM) content and spectral signatures, using bromoform separation and FieldSpec 4 spectroradiometer equipment, respectively. The spectral signatures of beach samples with a high HM content were characterized and resampled for the Sentinel-2 application, employing the Spectral Angle Mapper (SAM) algorithm. Field validation and an unmanned aerial vehicle (UAV) survey confirmed surface placer occurrences and the SAM's results. Santa Marta Beach exhibited significant placer anomalies (up to 30% HM), correlating with low SAM values (minimum value–0.10), indicating high spectral similarity. The SAM-derived anomaly patches aligned with the field observations, demonstrating Sentinel-2's potential for placer deposit mapping. This work highlights the application of Sentinel-2 in the exploration of placer deposits and the use of a specific spectral range of these deposits in coastal environments. These tools are non-invasive, more environmentally friendly, and sustainable, and can be extrapolated to other regions of the world with similar characteristics.

Keywords: spectral angle mapper; placer deposit; heavy minerals; Sentinel-2; laboratory reflectance spectroscopy; critical raw materials

Academic Editor: Konstantinos Topouzelis

Received: 14 March 2025
Revised: 11 May 2025
Accepted: 19 May 2025
Published: 23 May 2025

Citation: Ng-Cutipa, W.L.; Lobato, A.; González, F.J.; Georgalas, G.P.; Zananiri, I.; Carvalho, M.; Cardoso-Fernandes, J.; Somoza, L.; Piña, R.; Lunar, R.; et al. Spectral Angle Mapper Application Using Sentinel-2 in Coastal Placer Deposits in Vigo Estuary, Northwest Spain. *Remote Sens.* **2025**, *17*, 1824. https://doi.org/10.3390/rs17111824

1. Introduction

Marine placer deposits are accumulations of heavy minerals found on beaches and shallow seafloors in coastal areas. These deposits are commonly sources of economically valuable minerals and elements such as gold and diamonds, but also titanium (ilmenite, rutile, and anatase) and zirconium (zircon), with by-products of rare earth elements (monazite and xenotime) and tin (cassiterite), among others [1–3]. Many of the metals contained in these minerals are considered strategic or critical for the development of high technology and clean energy in Europe [4]. Given the complexity and mineralogical diversity, as well as

the size and location of these deposits in areas affected by tides, currents and waves, there are still limited Earth Observation (EO) studies applied to the exploration of these resources. Added to this is the diversity of satellites with multi- and hyperspectral characteristics and the different spectral response of minerals (heavy and light) separately ([5]; Figure 1), as well as their inclusion in mixed samples, which is how they are found in nature. In beach placer deposits, satellite exploration efforts have focused mainly on the search for titanium minerals, such as ilmenite [6–8]; zirconium sources, such as zircon [7,8]; iron sources, such as magnetite [7,9–12]; and rare earth elements (REEs), such as monazite [7,11].

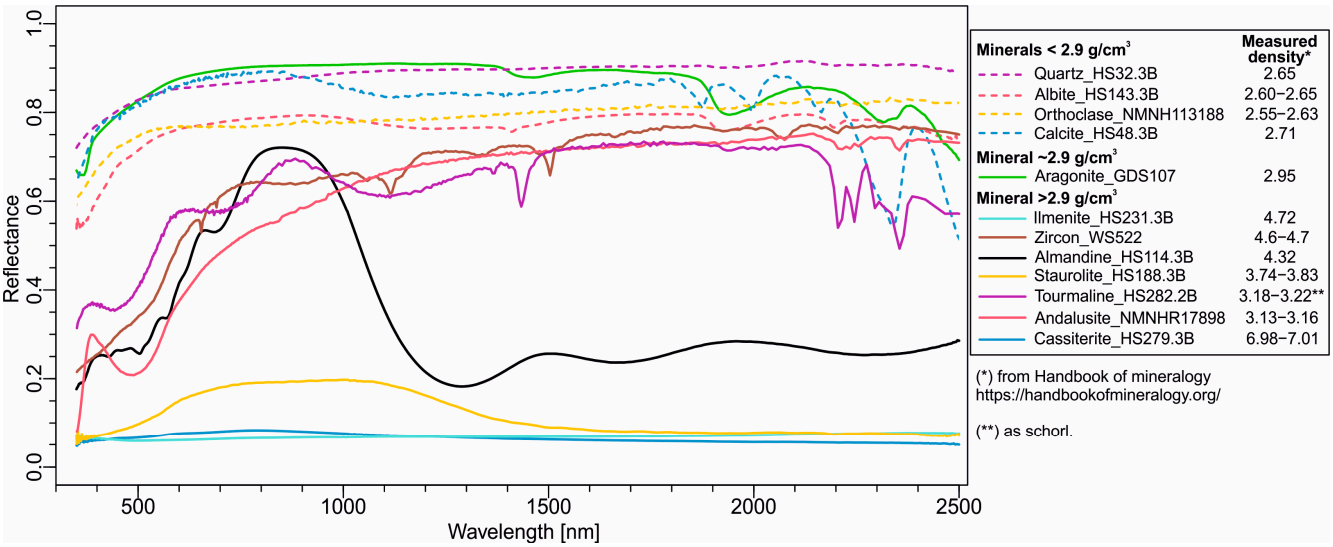

Figure 1. Spectral signature of light (<2.9 g/cm^3) and heavy (>2.9 g/cm^3) minerals that form barren and heavy mineral sands. Density data from Handbook of Mineralogy web (https://handbookofmineralogy.org/, accessed on 6 May 2025). The signatures are from the USGS Spectral Library [5].

In the Rias Baixas, a group of estuaries in NW Spain, previous systematic studies have revealed the existence of coastal placer occurrences on beaches and in shallow waters, such as those compiled by the GSEU project (European Critical Raw Materials Maps, available in https://www.geologicalservice.eu/upload/content/1753/egs_gseu_all_crm_maps.pdf, accessed on 6 May 2025) and others [13–16]. These studies had the limitation of reporting qualitative and semi-quantitative data. In the last two years, in the Vigo Estuary, the southernmost of the Rias Baixas, placer deposits have been studied with novel field, laboratory, and EO techniques within the framework of the European project S34I (https://s34i.eu/, accessed on 10 March 2025).

This work aims, among other objectives, to explore the use of bulk beach samples with different heavy mineral contents to assist in the search for critical raw materials for the energy transition by applying EO techniques in coastal and shallow-water areas. Thus, this project employs non-invasive tools that are more responsible and sustainable for the environment but also can be extended to other regions of the world. This work shows, for the first time, the characteristics of the spectral signatures of beach samples with and without heavy minerals in the Vigo Estuary, allowing us to develop a multi-scale methodology for mapping marine placers using the Spectral Angle Mapper (SAM) algorithm on Sentinel-2 images, and unmanned aerial vehicle (UAV) flights on Limens and Santa Marta beaches.

2. Study Area

The Vigo Estuary is located on the NW coast of Spain, in the Galicia region. It has a NE-SW orientation (Figure 2), where the Verdugo River discharges its freshwater into the Atlantic Ocean. Regionally, the estuary is surrounded by igneous (granites) and metamorphic (mainly gneisses and schists) rocks of the Paleoproterozoic to Jurassic age [17], in which evidence of placers has been reported [13–15]. Recently, within the framework of the S34i project (https://s34i.eu/, accessed on 10 March 2025), this estuary has been the pilot area for the exploration of critical raw materials in shallow water. The estuary has traditionally been divided into an inner part (where the main freshwater input occurs through the main drainage), a middle part, and an outer part (with more marine influence; [18]).

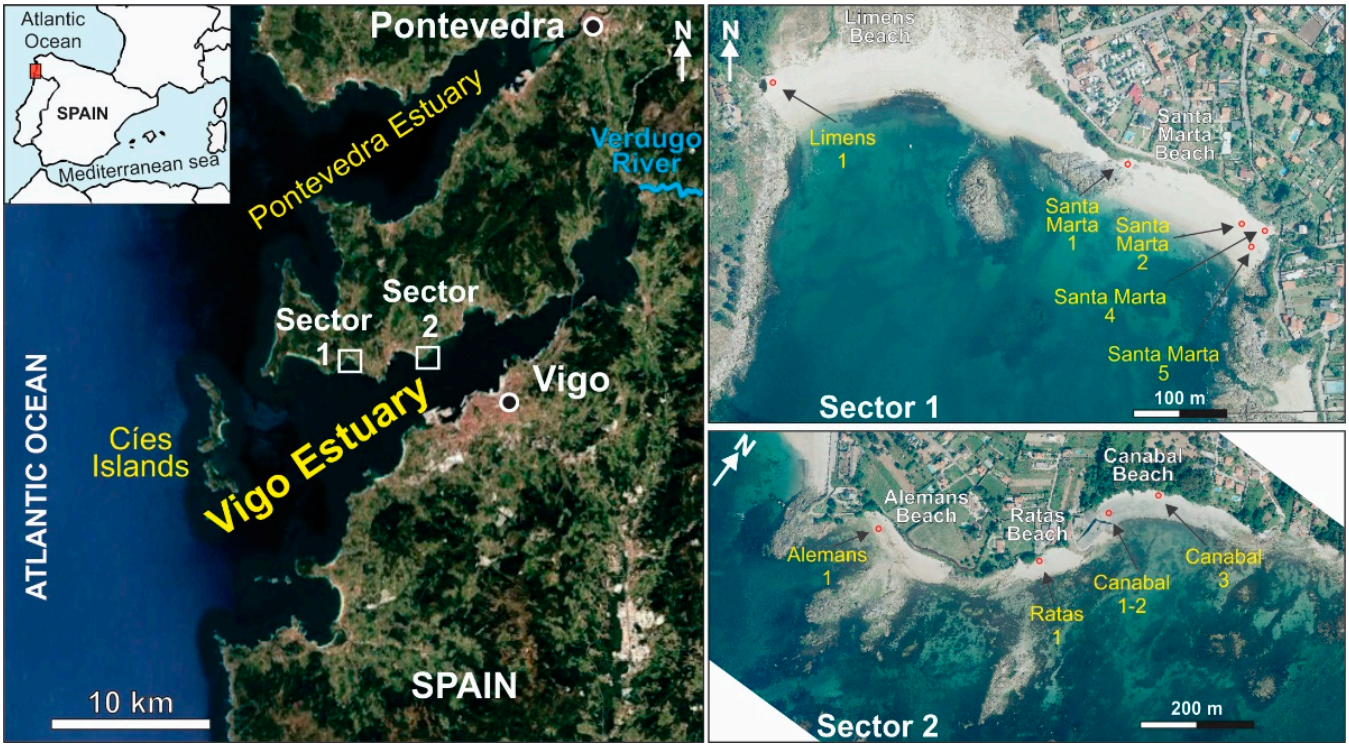

Figure 2. Situation of Vigo Estuary (Google Earth, https://www.google.es/intl/es/earth/index.html, accessed on 3 February 2025) and sand samples in Sector 1, Limens and Santa Marta beaches, and Sector 2, Alemans, Ratas, and Canabal beaches (National Aerial Orthophotography Plan-PNOA, https://pnoa.ign.es/web/portal/inicio, accessed on 10 September 2024).

Multiple short-course ephemeral streams are activated during rainy periods, from November to April (www.climate-data.org, accessed on 21 February 2025), during which they drain and transport sediments from the upland mountains into the estuary. Intertidal variations in the Atlantic zone of Galicia range from 2 to 3 m above sea level [18]. The study area is divided into two sectors in the middle part of the estuary: one formed by the Limens–Santa Marta beaches, and the other by the Alemans, Ratas, and Canabal beaches. Sector 1 (Figure 2), the Limens–Santa Marta beaches, is located about 8 km NE of the city of Vigo, where ilmenite, zircon, garnets, and other heavy minerals have been reported [13–15,19,20]. Recent studies within the S34i project have shown that surface placers are located in the intertidal zone, mainly occupying the beach face, although they are also occasionally found on the backshore [21]. Likewise, Sector 2 (Figure 2), formed by the Alemans, Ratas, and Canabal beaches, is about 4 km E of Sector 1 on the same side of the estuary, where no accumulations of heavy minerals of interest have been reported. In addition, a recent effort

to explore placer deposits using remote sensing was conducted in [22] using band ratios (involved in the S34I project).

3. Materials and Methods

3.1. Workflow

To achieve the objective, we completed five tasks using a workflow (Figure 3). Step 1 corresponded to the sampling and initial recognition of the reference area size of heavy minerals in both sectors, as well as their location with respect to the beach (beach face and backshore), rocky outcrops, and enriched layers of heavy minerals in the subsurface. Step 2 was performed in the laboratory, performing the measurement of the spectral signatures of the samples collected in the field. Step 3 consisted of a field trip to validate surface placers on the ground. Step 4 involved choosing the Sentinel-2 image temporally coincident with the field trip and to apply the subset and resampling routine. Finally, in step 5, the Normalized Difference Water Index (NDWI) was calculated, and the SAM algorithm was applied in Sector 1, using the two spectral signatures of samples with high heavy mineral contents (Santa Marta 4 and 5, Table 2).

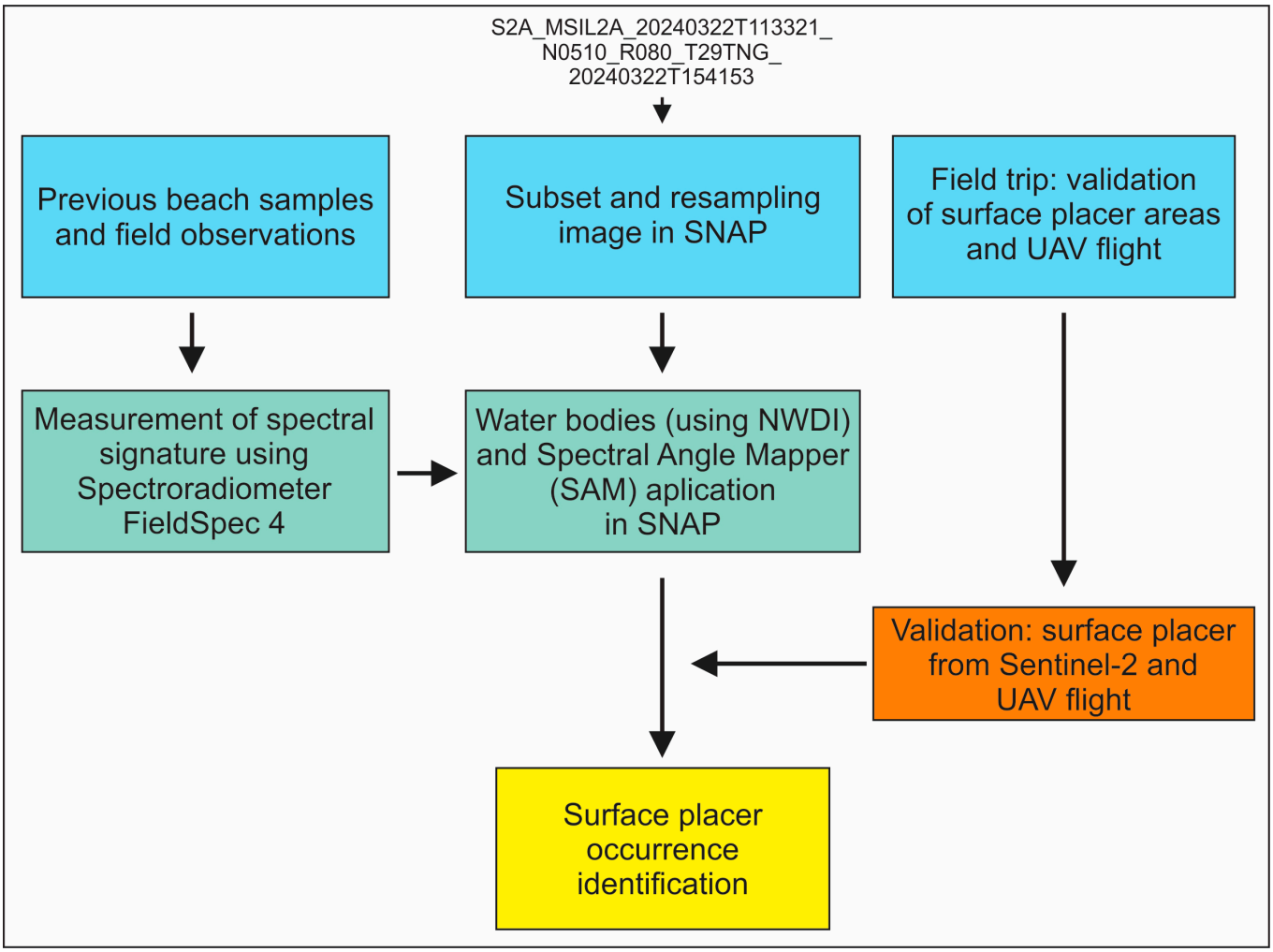

Figure 3. Flowchart for detecting placer occurrences using field data and multispectral images from Sentinel-2.

3.2. Beach Samples, Heavy Minerals and Spectral Signature Measurement

Ten sediment samples were collected from intertidal beach areas within the Vigo Estuary (Figure 2) during March 2023 (Limens 1, Santa Marta 1–2, Santa Marta 4, Alemans

1, Ratas 1, Canabal 1–3), except for one sample collected in September 2023 (Santa Marta 5). Samples were obtained from the uppermost centimeter of surface sand sediments. As previously demonstrated by [19], heavy mineral accumulations are not uniformly distributed across the beach, but rather occur as isolated patches, typically covering an average area of approximately 50 m^2, located on the backshore and beach face. The heavy mineral content in the fine sand fraction of these 10 samples has been previously analyzed. It included almandine, ilmenite, zircon, tourmaline, andalusite, staurolite, cassiterite, and others [20]. These minerals were determined by XRD. Bulk mineralogical XRD diffractograms from $2\theta = 2–70^\circ$ in 0.005 steps were obtained of the sandy samples using a PANalytical X'PERT PRO diffractometer (Philips Analytical, Almelo, The Netherlands), Cu-Kα radiation (40 kV and 40 mA) with a graphite monochromator, the software High Score version 3.0.4, and the ICDD and COD databases.

Approximately 50 g of each bulk sample, previously subjected to a drying process at a temperature of 45 °C (for a duration of approximately 24 h), underwent dense liquid separation at the IGME Laboratory (Madrid). A subsample was introduced into a separation funnel pre-filled with pure bromoform (density: 2.9 g/cm^3). Heavy and light minerals were separated based on their density, with heavy minerals settling at the bottom. The separated heavy and light mineral fractions were then collected on individual filter papers. This procedure was repeated, and the final heavy and light mineral fractions were weighed to determine their respective percentages.

Additionally, a separate subsample from each bulk sample was utilized for spectral library development. Spectral data were acquired at the Institute of Earth Sciences (University of Porto) using a FieldSpec 4 standard resolution spectroradiometer (ASD Inc., Boulder, CO, USA), covering the 400 to 2500 nm spectral range with three sensors (two for SWIR, and one for VNIR). The spectral acquisition was conducted in a dark room after ensuring the three sensors of the equipment were at the same temperature (after heating for 30 min). The equipment has a Contact Probe with an internal light source provided by a halogen bulb and a spot size of 10 mm that was used for taking the measurements. First, the normalization was made using perfect albidum (with plate) with reflectance equal to 1. The samples were positioned in a Petri dish, and the spectra were collected. All spectra consisted of the average of five measurements taken at the same spot in the sample. Each raw spectrum measurement was normalized using the continuum removal technique with a Python v2.7.10 script according to [23]. The average spectrum was automatically calculated using the Indico Pro v6.5.6.1 software during the acquisition process [24].

3.3. Sentinel-2 Data, NDWI, and SAM

Sentinel-2 images correspond to 22nd March 2024, (S2A_MSIL2A_20240322T113321_N0510_R080_T29TNG_20240322T154153). We used data acquired at level 2 of processing (with atmospheric correction and surface reflectance computation), which allowed us to use the image directly. Band specifications, spatial resolution, and wavelength ranges are detailed in Table 1. The original Sentinel 2 image was subsetted to consider the Santa Marta area, and the bands were resampled at a rate of 10 m per pixel, using the Sentinel Application Platform (SNAP, available at https://earth.esa.int/eogateway/tools/snap, accessed on 20 September 2024).

The NDWI was calculated using bands 3 and 8 of the Sentinel-2 dataset, following the methodology of [25]. NDWI values exceeding 0.2 were interpreted as indicative of water bodies, whereas values between 0 and 0.2 were associated with submerged vegetation, and soil–water and rock–water interfaces.

Table 1. Sentinel-2 band specifications.

Band	Resolution (m)	Wavelength Range (nm)	Central Wavelength for S2A (nm)
1	60	433–453	442.7
2	10	458–523	492.7
3	10	543–578	559.8
4	10	650–680	664.6
5	20	698–713	704.1
6	20	733–748	740.5
7	20	773–793	782.8
8	10	785–900	832.8
8A	20	855–875	864.7
9	60	935–955	945.1
10	60	1360–1390	1373.5
11	20	1565–1655	1613.7
12	20	2100–2280	2202.4

Data available in https://sentiwiki.copernicus.eu/web/s2-mission (accessed on 24 February 2025).

The SAM algorithm, widely employed in geological and environmental studies, was utilized to assess spectral similarity between pixels. SAM calculates the angular difference between two spectra, producing a pixel-wise classification ([26]; Figure 4). NDWI and SAM operations were employed using SNAP.

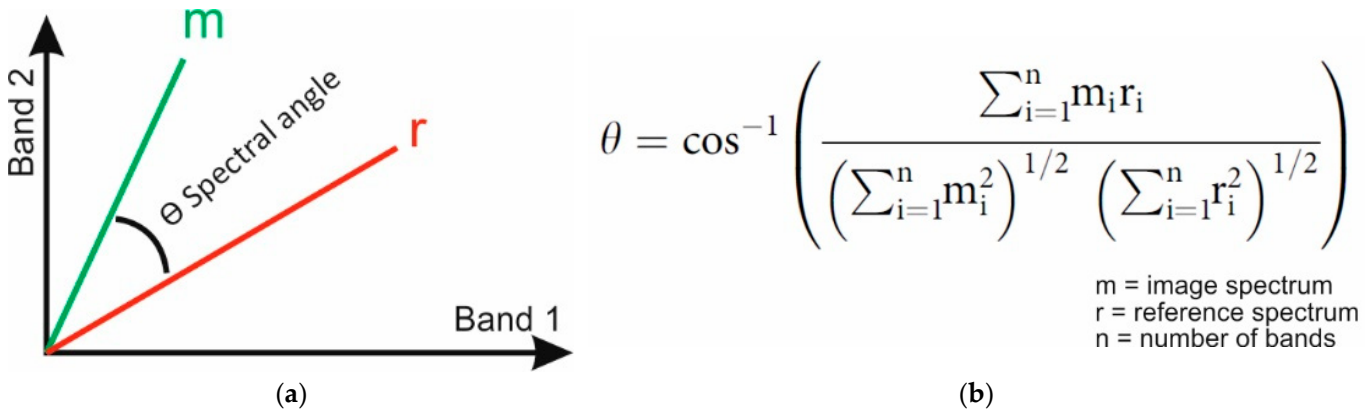

Figure 4. (**a**) Schematic of SAM principles, and (**b**) formula for calculations considering n bands [26].

For SAM analysis, the average spectrum of each sample was resampled using ENVI 6.1 (https://www.geospace-solutions.com/envi, accessed on 3 February 2025) to match the 12 bands of Sentinel-2, including band 8A. Multiple SAM values (radians) were evaluated to identify the thresholds, with 0.01 increments from the calculated minimum, to determine the optimal value for identifying placer deposits.

Initially, the threshold was tested with SAM values greater than 0.20, without finding isolated matches; on the contrary, the entire beach was within these values. Observing the minimum value, we tested several ranges, finding a threshold of 0.12 for the similarity value, with high spatial correlation between the Sentinel-2 results and the field data. Subsequently, we analyzed the data between the minimum value and the threshold of 0.12 for both field spectral signatures, establishing three similarity ranges: range 1 from the minimum value to 0.10 (lower SAM values; therefore, greater similarity), range 2 from greater than 0.10 to 0.11, and range 3 from greater than 0.11 to 0.12.

3.4. Validation Using In Situ Data

A field campaign was conducted on 19 March 2024 with two primary objectives. Firstly, an orthorectified RGB image was acquired via a UAV survey utilizing a DJI Mini 2 drone operated by the Hellenic Survey of Geology & Mineral Exploration (HSGME, http://www.eagme.gr, accessed on 10 March 2025). The equipment used GPS+GLONASS+GALILEO for the Global Navigation Satellite System, and had a 1/2.3″ CMOS sensor with an effective pixel of 12 MP (detailed specifications in https://dofly.com.pk/dji-mini-2-specs/, accessed on 5 May 2025). The camera does not capture spectral information beyond the visible range. Two flights were executed at altitudes of 80 (560 photos) and 50 (431 photos) meters, yielding a spatial resolution of 0.023 and 0.014 m, respectively. The flights were operated using the Map Pilot Pro application from Maps Made Easy. Flight parameters were as follows: image overlap = 75%, cover type = normal, and ground offset = 0 m. Photogrammetric processing was carried out using Agisoft Metashape Professional 2.2.1. Additionally, six control points were collected using differential GPS and were distributed throughout the entire area to be surveyed by the drone. The points were marked on the ground with removable materials to facilitate their identification in the imagery. The final orthorectified image data were used to delineate placer polygons within the study area. Secondly, surface patches of heavy minerals were identified and compared with data from previous field surveys.

4. Results

4.1. Heavy Mineral Content

The analysis revealed that most samples contained less than 6% heavy minerals by weight. Samples from Santa Marta 2, Santa Marta 4, and Santa Marta 5 exhibited higher concentrations, exceeding 10% (Table 2).

Table 2. Heavy mineral quantification in sand samples from Vigo Estuary.

Nº	Sample	Light Minerals (g)	Heavy Minerals (g)	Light Minerals (%)	Heavy Minerals (%)
1	Limens 1	51.97	0.86	98.37	1.63
2	Santa Marta 1	43.98	1.65	96.38	3.62
3	Santa Marta 2	45.38	5.56	89.01	10.91
4	Santa Marta 4	45.92	6.69	87.28	12.72
5	Santa Marta 5	8.13	19.42	70.49	29.51
6	Alemans 1	49.64	0.69	98.63	1.37
7	Ratas 1	47.48	2.74	94.54	5.46
8	Canabal 1	48.55	1.47	97.06	2.94
9	Canabal 2	39.7	1.43	96.52	3.48
10	Canabal 3	50.56	1.58	96.97	3.03

Specifically, Santa Marta 2 (11% heavy minerals) displayed a surface accumulation of dark minerals in the central beach area (Figure 5), attributed to recent wave deposition. Santa Marta 4 (13% heavy minerals) showed reddish to dark minerals originating from a small ephemeral drainage in the southeastern portion of the beach (Figure 5). This backshore accumulation indicates active heavy mineral transport into the beach system via the stream. Santa Marta 5 (30% heavy minerals) exhibited a higher concentration of reddish heavy minerals than Santa Marta 4, located on the beach face (Figure 5).

Figure 5. Field trip images of placer distribution. Surface heavy minerals on Santa Marta Beach, beach face (Santa Marta 2 and 5), and backshore (Santa Marta 4).

4.2. Spectral Signature of Sand Samples

The reflectance of the samples was measured continuously from 400 to 2500 nm (Figure 6a). In general, the spectral signatures have a similar trend between 400 and 1000 nm, distinguished by the average reflectance values. These spectral signatures show three main regions of absorption, at around 1400, 1900, and 2200 nm (Figure 6a), corresponding to OH/water, water, and Al-OH absorption features, respectively [27]. Samples Santa Marta 4 and 5 are distinguished from the others by a lower average reflectance. In these, the spectral signature decreases from 1000 nm to just before the first minimum (approximately 1400 nm), and remains semi-horizontal up to 2500 nm, with slight, very specific changes. In Santa Marta, it is observed that the higher the heavy mineral content, the lower the average reflectance values (as in Santa Marta 5).

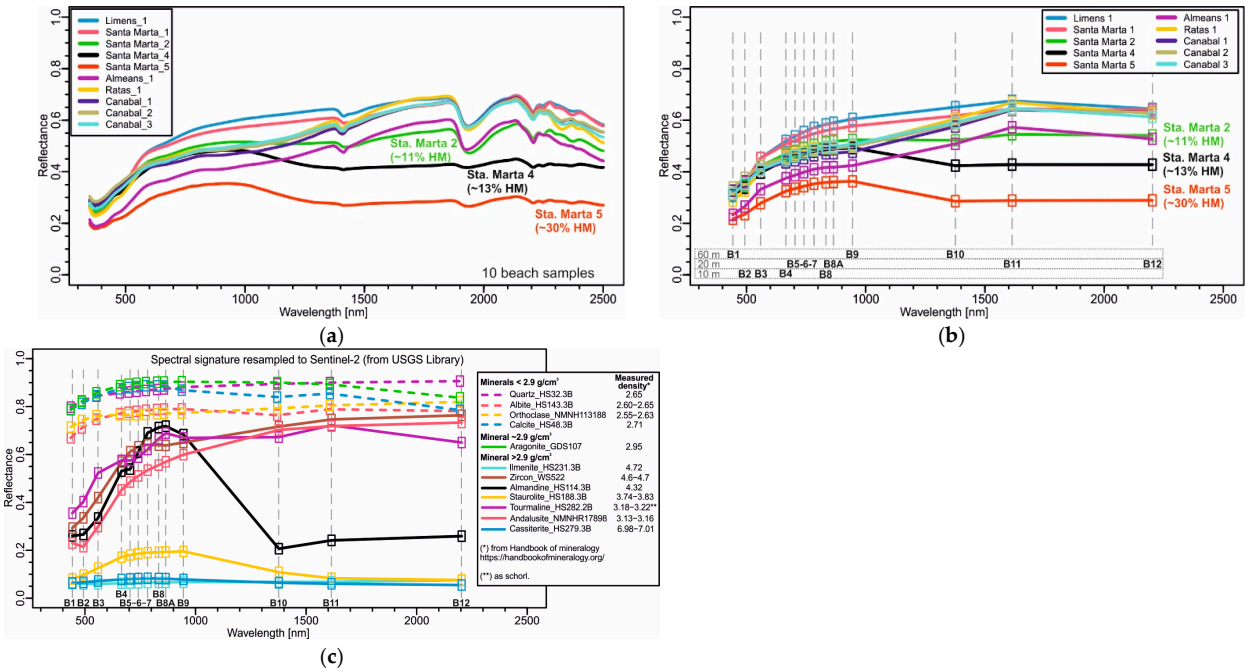

Figure 6. Spectral signatures of beach samples in (**a**) continuous measurement with the FieldSpec 4 spectroradiometer, (**b**) resampled bands for Sentinel-2 used in this study, and (**c**) resampled bands of minerals to Senitnel-2 (from USGS Library: https://www.sciencebase.gov/catalog/item/5807a2a2e4b0841e59e3a18d, accessed on 16 January 2025).

When we resampled the original continuous spectral signatures with the Sentinel-2 bands, these signatures ascended to band 9 in all samples (Figure 6b). In this correlation, two groups are differentiated: the samples that continue with an increase in reflectance in bands 10 and 11, without a high heavy mineral content, and a second group with a decrease in band 10, which are those with ≥10% heavy minerals (Santa Marta 2, 4–5, Figure 6b). Bands 11 and 12 of these three samples remain practically horizontal. Another important feature is that the three main absorption features (around 1400, 1900, and 2200 nm) observed in the continuous spectral signature are lost. Furthermore, if we compare Figure 6b and the resampled spectral signatures of minerals from the USGS Spectral Library (Figure 6c, data available at https://www.sciencebase.gov/catalog/item/5807a2a2e4b0841e59e3a18d, accessed on 16 January 2025), the spectral signatures are different. We can observe that the spectral signature of beach samples with high 10% HM (Santa Marta 2, 4–5) has reflectance values similar to one group of minerals in B1–B9 (e.g., tourmaline, andalusite, almandine, and zircon) and similar to another group of minerals in B10–B12 (e.g., almandine and probably staurolite, ilmenite, and cassiterite). This pattern confirms that the samples are composed of more than one HM in predominance.

4.3. Water Body Measurements Using NDWI and SAM in SNAP

The application of the NDWI, considering ranges greater than 0.2 as water and between 0 and 0.2 as underwater plants (mainly algae) and boundaries with the emerged area of soils and rocks, shows a varied distribution. The calculations show that algae are found around the coastline, in addition to an isolated patch towards the center of the cove. Likewise, in front of the boundary of the Limens and Santa Marta beaches, the emerged rocky outcrop is clearly distinguished (Figure 7b). Furthermore, on the Limens and Santa Marta beaches, pixels with NDWI values between 0 and 0.2 represent the wave zone.

On the other hand, the SAM calculation using the spectral signatures of Santa Marta on the Sentinel-2 image shows very similar zones of placer deposits using the field spectral signatures of Santa Marta 4 and 5 (Figure 7c,d). In both calculations, range 1 of greatest similarity is found in the same pixel SE of Santa Marta Beach (Figure 7c), a preferential area of heavy mineral accumulation observed in previous field visits.

The SAM results using the Santa Marta 4 spectral signature show a minimum value of 0.092 (range 1, Figure 7c), which is located at the SE end of Santa Marta Beach. Values of range 2 (>0.10–0.11, Figure 7c) are found NW of the minimum value and isolated SE of Limens Beach. Values of range 3 (>0.11–0.12, Figure 7c) are found on both beaches, more continuously on Limens and isolated on Santa Marta. The two accumulations of range 3 pixels on Limens Beach are elongated and parallel to the shoreline but are not immediately adjacent to the land–sea boundary.

The SAM using the Santa Marta 5 spectral signature (Figure 7d) shows a spatial distribution very similar to that of Santa Marta 4. The minimum value is 0.086 (range 1 in red, Figure 7d) in this calculation, and is of greater similarity and occurs in the same pixel as when using Santa Marta 4. Range 2 (>0.10–0.11, Figure 7d) is shown in non-continuous pixels on Santa Marta Beach and SE of Limens. A new pixel of this range, along with several aligned pixels (which have changed range with respect to the Santa Marta 4 spectral signature), are found on Limens Beach. Regarding range 3 (>0.11–0.12, Figure 7d), two new pixels are recognized SW of the minimum value (range 1) on Santa Marta Beach and a new pixel W of Limens Beach. Furthermore, this range represents a lateral transition on each side of the continuous pixels of range 2 on Limens Beach.

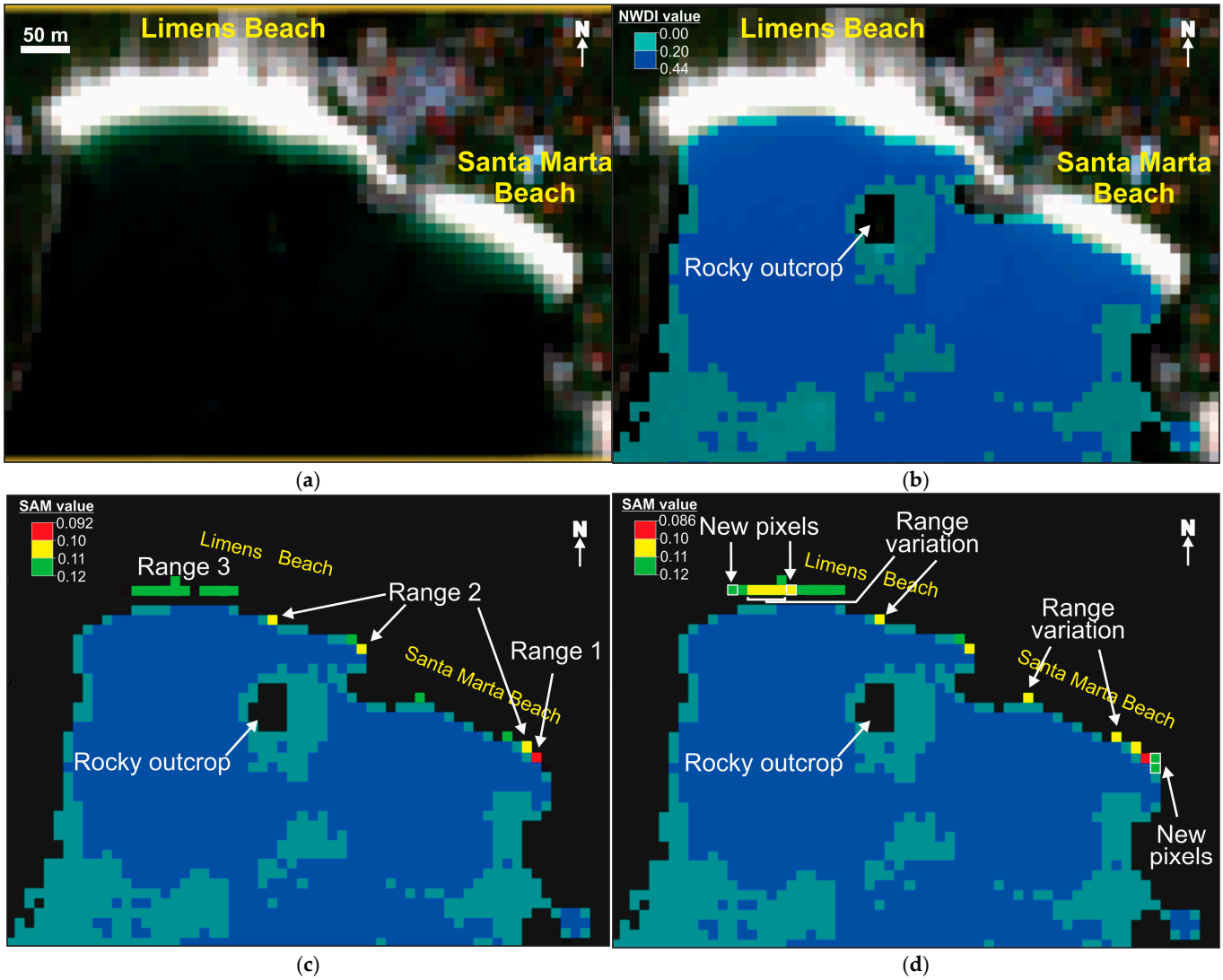

Figure 7. Sentinel-2 image in (**a**) true color composite, (**b**) NWDI calculated using values greater than 0.2 and 0–0.2, (**c**) NWDI and SAM calculation using Santa Marta 4 spectral signature, and (**d**) NWDI and SAM calculation using Santa Marta 5 spectral signature. SAM values from minor to major similarity: minimum–0.10 (red), 0.10–0.11 (yellow), and 0.11–0.12 (green).

The SAM results show a greater similarity (lower SAM values) SW of Santa Marta Beach, which is the same area where heavy minerals have been observed on the surface in previous field trips in 2023 and 2024. They also show areas with discontinuous pixels on Santa Marta Beach (mainly towards the SW) that are adjacent to the shoreline, and with continuous and elongated pixels on Limens Beach that are not immediately adjacent to the land–sea boundary. In addition, there is greater similarity using the Santa Marta 5 spectral signature.

4.4. Validation Using UAV Survey

The field visit allowed us to find surface placers again with a higher concentration on Santa Marta Beach (Figure 8), as well as the formation of an ephemeral drainage that brings heavy minerals towards the sea from inland. This stream also erodes the previous levels of placers accumulated in the subsurface of the SW part of the beach (Figure 8), taking them to the shoreline, where tides and waves act.

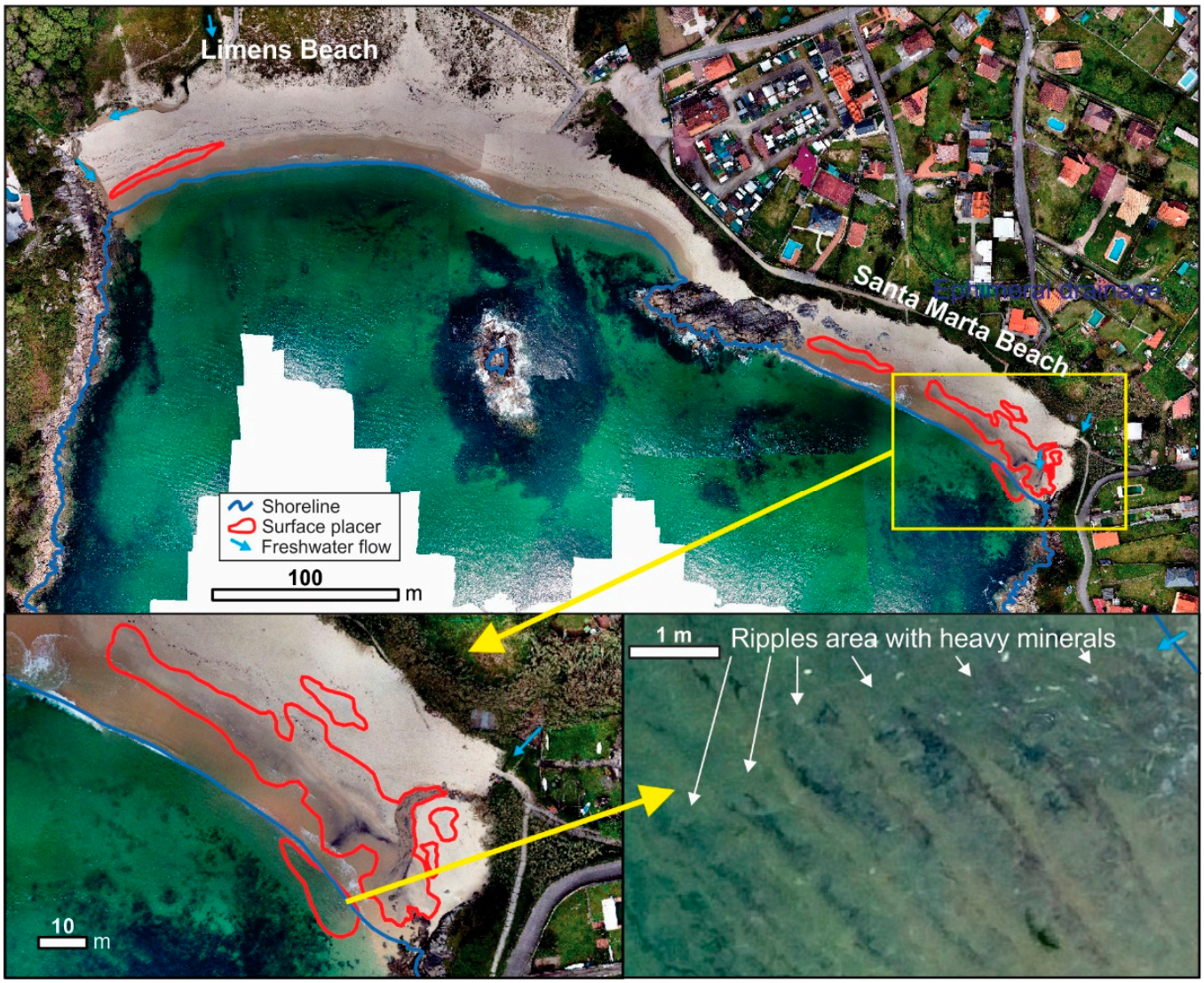

Figure 8. Surface placer occurrence bodies in Limens and Santa Marta beaches. Most surface heavy minerals are SW of Santa Marta Beach. At the mouth of the ephemeral drainage, it is possible to identify heavy mineral accumulation in ripples (shallow water areas). UAV images from the validation field trip (19 March 2024).

Geographical Information System (GIS) mapping based on UAV data has allowed us to identify six areas with surface placers on Santa Marta Beach, and one on Limens Beach (Figure 8). The extension ranges from 12 to 948 m^2, in which the concentration of heavy minerals decreases towards the outside of each polygon. These patches of heavy minerals are mainly in the upper part of the intertidal zone and appear to be elongated parallel to the shoreline in the UAV. An accumulation of heavy minerals in the ripple zone in shallow water has been found (Figure 8) at the mouth of the ephemeral drainage (Figure 9).

Our results show that there is an appreciable spatial correlation between the surface placers calculated by the SAM algorithm in Sentinel-2 and the field mapping using UAV data, highlighting that the greatest similarities with the field spectra used are found SW of Santa Marta Beach (Figure 10).

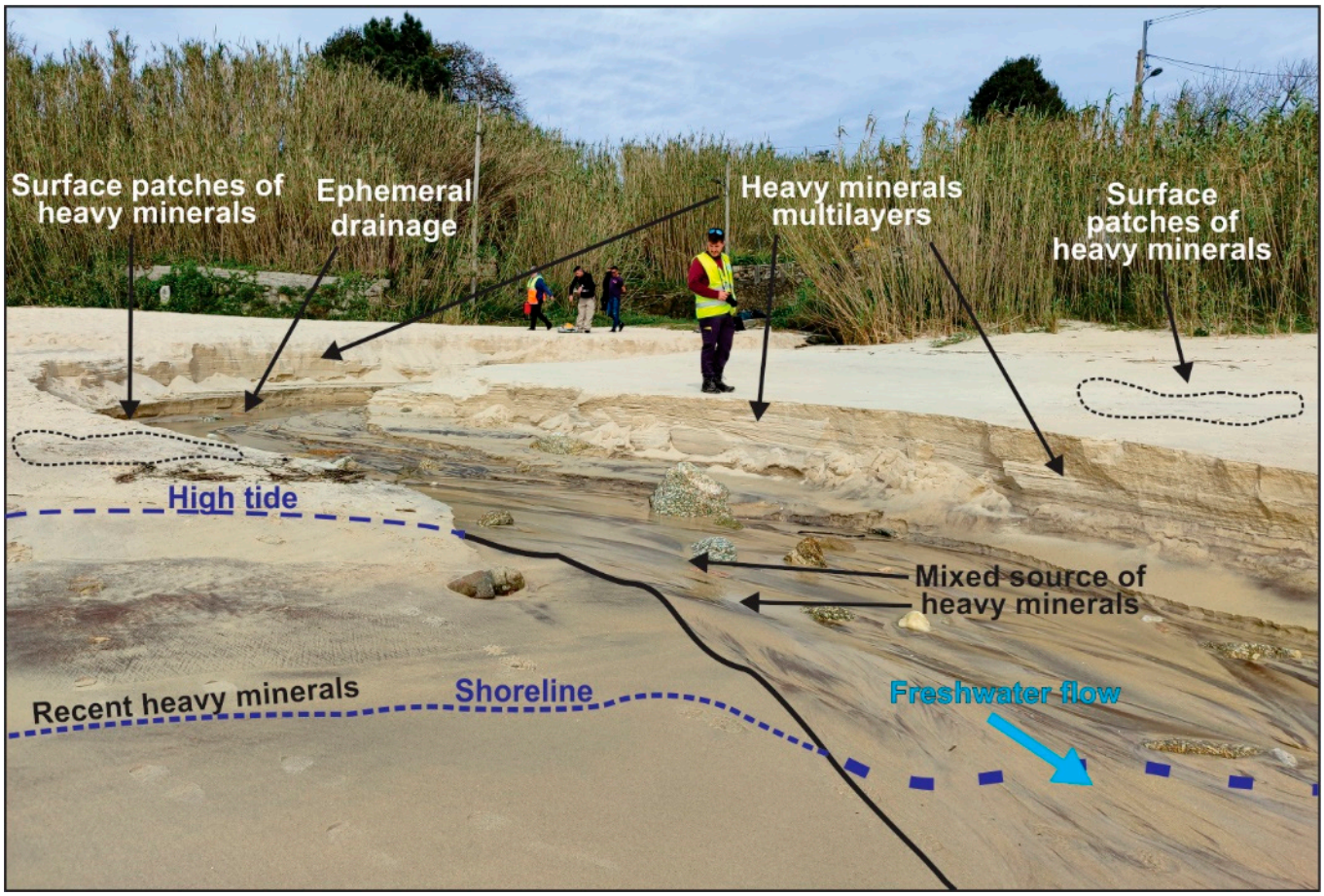

Figure 9. Detailed image of surface placer occurrence and multilayer accumulation of heavy minerals in subsoil around the ephemeral drainage SW of Santa Marta Beach (field trip validation).

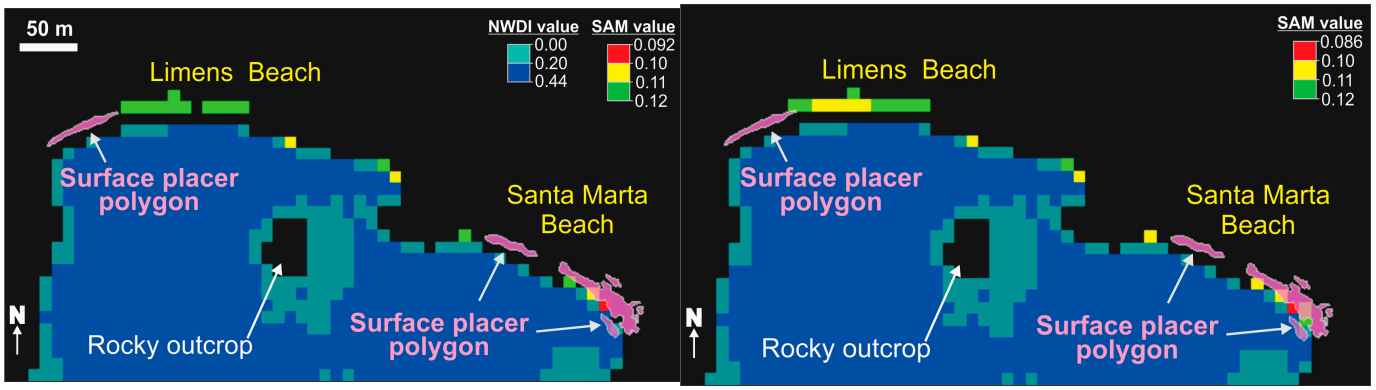

Figure 10. Overlapping surface placer areas from the UAV survey (purple polygons) in (**a**) water body boundaries and SAM using Santa Marta 4 spectra from Sentinel-2, and (**b**) water body boundaries and SAM using Santa Marta 5 spectra from Sentinel-2. The major similarity (lower SAM value, using both spectra) is located to the east of Santa Marta Beach, which is also the preferred location where the heavy minerals observed during the field campaigns are concentrated.

5. Discussion

5.1. Integrating In Situ Surface Placer Data with EO Data

Laboratory studies of heavy minerals provide a good starting point for characterizing the spectral signatures of samples containing placer deposits. In the study area, the reported heavy minerals are mainly almandine, staurolite, and ilmenite [19–21]. According to the

spectral signature library [5], these minerals have a reflectance of less than 0.3 (Figure 1) after 1100 nm. This could explain why mixed samples with >13% heavy minerals (especially in Santa Marta 4 and 5) are distinguished from the rest of the placer-free samples by (1) lower reflectance values throughout the spectrum, and (2) semi-horizontal reflectance values after 1400 nm (Figure 6a).

Furthermore, the results of this study show that samples Santa Marta 4 and 5 (13 and 30% heavy minerals, respectively) exhibit a reflectance decrease between 1000 and 1400 nm, a characteristic that can be exploited by remote sensing techniques. In addition, the higher the heavy mineral content, the lower the reflectance magnitude values, maintaining its curvature. This lower reflectance magnitude and the relatively flat behavior in the SWIR region could be a direct consequence of the higher heavy mineral content since some of these heavy minerals, such as ilmenite, are typically opaque on reflectance spectroscopy, while others, like garnets (almandine) and staurolite, show strong general absorption to both long and short wavelengths, where the reflectance maximum is achieved well before 1100 nm (850 nm for almandine and 1050 nm for staurolite; [5,28,29]). On the other hand, other satellite resources that include spectral bands covering between 1000 and 1400 nm could help to better detect anomalies of this type of placers.

The NWDI calculation has served to locate the boundary between the water body and the beach above sea level, where placer deposits have been observed.

The SAM results, tested every 0.01, have allowed us to establish 0.12 as a threshold. This value is like those found by [12], between 0.12 and 0.17. The SAM values obtained using the spectral signatures of samples Santa Marta 4 and 5 have a similar pattern in the distribution of anomalies using the same threshold (minimum value–0.10, >0.10–0.11, and >0.11–0.12).

This threshold value of 0.12 may be due to the mineralogical complexity of the placer but also to the final pixel size (10 × 10 m) and the bands (number of bands and their spectral range) of Sentinel-2. The sand samples collected in the field could represent the central part of the placer patches within the 10 × 10 m pixels that have an average signature of that area. In addition, the spectral signatures of bands B9 and B10 in these resampled Sentinel-2 pixels represent averages of larger areas (60 m originally), where we have seen a decrease in the reflectance in the placer samples (Santa Marta 4 and 5, Figure 6).

The validation has shown a high spatial correlation of placer anomalies in the Limens and Santa Marta beaches (Figure 10). However, there are segments where the mapping and SAM anomalies do not coincide spatially, such as in the central and eastern parts of Limens Beach. This could be due to the high dynamics of the distribution and accumulation of heavy minerals in coastal areas, mainly due to intertidal action and waves, which occurred within the 3-day temporal offset between the UAV flight and the Sentinel-2 image used.

On the Limens and Santa Marta beaches, two characteristics of placer distribution have been verified, both through field observations (previous and validation using UAV shown in this study) and those obtained using Sentinel-2. The first is that the highest placer contents are SW of Santa Marta Beach (Figures 8–10), with greater similarities in the SAM calculation (Figure 7c,d); and the second is that the anomalies are elongated parallel to the shoreline, continuous, and discontinuous segments of anomalies on Limens Beach (Figures 7c,d, 8–10).

This discontinuity of the surface placer areas has also been observed in other placer deposits [2,3,12], in Galician estuaries [13,15], and in this beach area in previous studies [19]. As previously stated, the reason for the presence of discontinuous patches of placers in the intertidal zone is mainly due to wave and tidal action.

5.2. Remote Sensing Applications to Explore Placer Deposits

As previously noted, heavy mineral assemblages typically consist of complex mixtures of heavy and light minerals, exhibiting considerable variations in lateral extent and vertical distribution. Multiple minerals may predominate in the heavy mineral fraction even when focusing on a specific commodity within a placer deposit. Furthermore, coastal environments are dynamic, characterized by shoreline fluctuations within the intertidal zone, with constraints for remote sensing applications.

Consequently, there are scarce publications detailing the application of remote sensing to explore placer deposits in coastal areas. Relevant works include [6–12,22]. These studies primarily utilize regional surveys such as ASTER (15–90 m spatial resolution) and Landsat (30–60 m spatial resolution), with less frequent use of EO-1 Hyperion (30 m spatial resolution). Only [22], employing Sentinel-2 for comparison with Landsat, and [12], utilizing a UAV with a six-band multispectral camera, present results at medium and high spatial resolutions, respectively.

Moreover, these studies often simplify and do not include factors that influence the spectral signature of placer deposits. For example, some investigations have considered a single heavy mineral [12], while others have accounted for mixed heavy minerals in field samples [8,11] and spectral responses [8]. In some instances, the percentage of heavy minerals in sand samples remains unknown [6,12]. Limited research utilizes spectral signatures from local samples ([6] shows one placer spectral signature, and [7] shows individual mineral spectral signatures) for validation and comparison. Most studies employ the SAM algorithm [6] or other algorithms [6–8,11], including artificial intelligence and machine learning [12], while others utilize band ratio analysis [10,22] to identify heavy minerals. Another factor influencing the spectral signature in coastal areas is the water content of the sand. The authors of [30] compare the spectral signatures of dry and wet sands (0–45% water content). Their results show that the spectral signature has lower values when the sample has a higher water content, while maintaining the curvature. We think this specific influence could affect the heavy mineral accumulation in the swash zone at the moment that the satellite data are collected. However, considering the UAV survey (Figure 8), the swash zone is from 5 to 12 m in length, and the majority of heavy mineral patches in our study area are located over the swash zones. Thus, taking into account the pixel size obtained from the resampling process (10 $\times$ 10 m), two spectral signatures with a high and low heavy mineral content, the location of heavy minerals, and the length of the swash zone, the identification of heavy minerals using the SAM technique provides robust results. In addition, our study is pioneering in that it uses the spectral signature of bulk samples from beaches with placer occurrences (approximate natural conditions) at a medium scale using Sentinel-2.

Therefore, our methodology and results address several gaps in the exploration of placer deposits using Sentinel-2 at a medium scale, specifically focusing on irregular patches of surface heavy mineral accumulations on small beaches. We emphasize the importance of (1) determining the percentage of heavy minerals in bulk samples, (2) utilizing multiple samples with varying heavy mineral contents to characterize and select appropriate spectral signatures, (3) considering the presence of multiple predominant minerals within the heavy mineral fraction (except for beaches totally composed by heavy mineral), and (4) the replicability of our study in similar areas.

6. Conclusions

This study focuses on the use of Sentinel-2 imagery and the Spectral Angle Mapper (SAM) algorithm to detect placer deposits on beaches in the Vigo Estuary, specifically on the Limens and Santa Marta beaches. Ten samples from five beaches (Limens, Santa

Marta, Alemans, Ratas, and Canabal) were analyzed, with two samples from Santa Marta Beach (samples 4 and 5) showing distinct spectral signatures due to high concentrations of heavy minerals (13% and 30%, respectively). These samples exhibited a significant decrease in reflectance between 1000 and 1400 nm, which became a key indicator for identifying placer deposits using remote sensing. The decrease in reflectance aligns with the spectral properties of heavy minerals known to occur in the study area.

By resampling the spectral signatures to match the Sentinel-2 bands, SAM was applied, with a threshold of 0.12 used to classify the spectral values. The SAM results revealed elongated placer zones in discontinuous patches on the beach face, which were consistent with field observations and UAV data, confirming the potential for the automated detection of placer deposits. These results highlight the importance of using heavy mineral-rich sample spectral signatures as key indicators for identifying placer deposits in coastal regions.

The study also found that placer deposits in the intertidal zone at Limens and Santa Marta were redistributed by wave and tidal action, with minimal spatial changes observed over a 3-day period. Sentinel-2 data, combined with higher-spatial-resolution resources like WorldView-3 and EnMap, could offer more precise identification of placer deposits. In the same way, subsequent studies that encompass temporal analysis and storm events have the potential to enhance the identification of heavy mineral behavior and the best time for their accumulation on the beach surface.

The study emphasizes the value of remote sensing for exploring coastal placer deposits in hard-to-reach areas, offering a non-invasive, environmentally sustainable method for resource exploration.

Author Contributions: Conceptualization, W.L.N.-C., A.L. and F.J.G.; methodology, W.L.N.-C., A.L., F.J.G., G.P.G., I.Z., M.C., J.C.-F. and A.C.T.; software, W.L.N.-C.; validation, W.L.N.-C., M.C. and G.P.G.; investigation, W.L.N.-C., A.L., F.J.G., L.S., G.G, I.Z, R.P., R.L., M.C., J.C.-F. and A.C.T.; data curation, W.L.N.-C., G.P.G. and M.C.; writing—original draft preparation, W.L.N.-C., A.L. and F.J.G.; writing—review and editing, W.L.N.-C., A.L., F.J.G., G.P.G., I.Z., M.C., J.C.-F., L.S., R.P., R.L. and A.C.T.; supervision, F.J.G., L.S., R.P., R.L. and A.C.T.; project administration, A.C.T.; funding acquisition, A.C.T. All authors have read and agreed to the published version of the manuscript.

Funding: This study is funded by the European Union under grant agreement no. 101091616 (https://doi.org/10.3030/101091616 (accessed on 24 February 2025)) project S34I—Secure and Sustainable Supply of Raw Materials for EU Industry, under topic HORIZON-CL4-2022-RESILIENCE-01-08–Earth observation technologies for the mining life cycle in support of EU autonomy and transition to a climate neutral economy (RIA). This work is also supported by national funds through FCT—Fundação para a Ciência e Tecnologia, I.P., in the framework of the UIDB/04683 and UIDP/04683—Instituto de Ciências da Terra programs.

Data Availability Statement: The Sentinel-2 images are available for free and were downloaded from https://browser.dataspace.copernicus.eu/ (accessed on 5 April 2024).

Acknowledgments: This work is a cooperation between the Instituto Geológico y Minero de España (IGME-CSIC), Universidad Complutense de Madrid (UCM), Hellenic Survey of Geology & Mineral Exploration (HSGME) and Institute of Earth Sciences, Faculty of Sciences of the University of Porto (UPorto). We also express our gratitude to Marta García for the laboratory work at IGME Labs. This study was also made possible thanks to the effort of the NGO's Guías de Espeleología y Montaña (GEM) and Canal de Isabel II.

Conflicts of Interest: The authors declare no conflicts of interest. The funders had no role in the design of the study; in the collection, analyses, or interpretation of the data; in the writing of the manuscript; or in the decision to publish the results. The views and opinions expressed are, however, those of the author(s) only and do not necessarily reflect those of the European Union or HADEA. Neither the European Union nor the granting authority can be held responsible for them.

References

1. Rona, P.A. The Changing Vision of Marine Minerals. *Ore Geol. Rev.* **2008**, *33*, 618–666. [CrossRef]
2. Van Gosen, B.S.; Fey, D.L.; Shah, A.K.; Verplanck, P.L.; Hoefen, T.M. *Deposit Model for Heavy-Mineral Sands in Coastal Environments*; Scientific Investigations Report; U.S. Geological Survey: Reston, VA, USA, 2014; p. 51.
3. Hou, B.; Keeling, J.; Van Gosen, B.S. Geological and Exploration Models of Beach Placer Deposits, Integrated from Case-Studies of Southern Australia. *Ore Geol. Rev.* **2017**, *80*, 437–459. [CrossRef]
4. European Commission. Directorate General for Internal Market, Industry, Entrepreneurship and SMEs. In *Study on the Critical Raw Materials for the EU 2023: Final Report*; Publications Office of the European Union: Luxembourg, 2023.
5. Kokaly, R.F.; Clark, R.N.; Swayze, G.A.; Livo, K.E.; Hoefen, T.M.; Pearson, N.C.; Wise, R.A.; Benzel, W.; Lowers, H.A.; Driscoll, R.L.; et al. *USGS Spectral Library Version 7*; Data Series; U.S. Geological Survey: Reston, VA, USA, 2017; p. 68.
6. Prates Hallal, G.; De Almeida Espinoza, J.M.; Veettil, B.K.; Porcher, C.C.; Oliveira Righi Da Silva, M.; Beatriz Alves Rolim, S. Mapping Heavy Mineral Deposits on the Coast of the State of Rio Grande Do Sul (Brazil) Using Orbital and Proximal Remote Sensing. *PLoS ONE* **2024**, *19*, e0309043. [CrossRef] [PubMed]
7. Rejith, R.G.; Sundararajan, M.; Gnanappazham, L.; Loveson, V.J. Satellite-Based Spectral Mapping (ASTER and Landsat Data) of Mineralogical Signatures of Beach Sediments: A Precursor Insight. *Geocarto Int.* **2020**, *37*, 2580–2603. [CrossRef]
8. Rejith, R.G.; Sundararajan, M.; Gnanappazham, L.; Kaliraj, S.; Chandrasekar, N. Exploring Beach Placer Minerals in the East Coast of Tamil Nadu, India, Using EO-1 Hyperion Data. *J. Appl. Remote Sens.* **2022**, *16*, 012017. [CrossRef]
9. Rao, K.J.; Subramanyam, A.V.; Abhinav Kumar, A.K.; Sunil, T.C.; Chaturvedi, A.K. Discovery of Heavy Mineral-Rich Sand Dunes along the Orissa-Bengal Coast of India Using Remote Sensing Techniques. *Curr. Sci.* **2008**, *94*, 983–985.
10. Putra, I.D.; Abbas, R.; Masti, S.D.; Warmada, I.W. Remote Sensing Application in Exploration of Iron Mineral Placer Deposit: Case Study of Kulonprogo's Iron Placer Deposit. In Proceedings of the EAGE-HAGI 1st Asia Pacific Meeting on Near Surface Geoscience and Engineering, Yogyakarta, Indonesia, 9–13 April 2018; European Association of Geoscientists & Engineers: Utrecht, The Netherlands, 2018; Volume 2018, pp. 1–5.
11. Rejith, R.G.; Sundararajan, M.; Venkatesan, S.; Mohammed-Aslam, M.A. Remote Sensing for Exploring Heavy Mineral Deposits. In *Remote Sensing of Ocean and Coastal Environments*; Elsevier: Amsterdam, The Netherlands, 2021; pp. 177–188, ISBN 978-0-12-819604-5.
12. Sinaice, B.B.; Owada, N.; Ikeda, H.; Toriya, H.; Bagai, Z.; Shemang, E.; Adachi, T.; Kawamura, Y. Spectral Angle Mapping and AI Methods Applied in Automatic Identification of Placer Deposit Magnetite Using Multispectral Camera Mounted on UAV. *Minerals* **2022**, *12*, 268. [CrossRef]
13. IGME. *Investigación Minera Preliminar de la Plataforma Continental Submarina del área sur de Pontevedra*; Programa Sectorial de Estudio de Fondos Marinos (FOMAR); Ministerio de Industria, Programa Nacional Investigación Minera, IGME: Madrid, Spain, 1976; p. 242.
14. IGME. *Investigación Minera de Detalle en los Fondos Submarinos de la zona de las rías de Pontevedra y Vigo (GALI-RIAS)*; Programa Sectorial de Estudio de Fondos Marinos (FOMAR); Ministerio de Industria, Programa Nacional Investigación Minera, IGME: Madrid, Spain, 1979; p. 83.
15. Manso, F. Exploración de Placeres Costeros de Minerales Pesados y su Génesis en la Costa de Galicia. Ph.D. Thesis, Universidad de Vigo, Vigo, Spain, 2001.
16. González, F.J.; Medialdea, T.; Schiellerup, H.; Zananiri, I.; Ferreira, P.; Somoza, L.; Monteys, X.; Alcorn, T.; Marino, E.; Lobato, A.B.; et al. MINDeSEA: Exploring Seabed Mineral Deposits in European Seas, Metallogeny and Geological Potential for Strategic and Critical Raw Materials. *Geol. Soc. Lond. Spec. Publ.* **2023**, *526*, 289–317. [CrossRef]
17. González, M.I.; Vicente, J. *Mapa Geológico de España con la Inclusión de Portugal Continental y Pirineos Franceses a Escala 1:2.000.000*; IGME: Madrid, Spain, 2004.
18. Vilas, F.; Bernabéu, A.; Rubio, B.; Rey, D. The Galician Rías. NW Coast of Spain. In *The Spanish Coastal Systems: Dynamic Processes, Sediments and Management*; Morales, J.A., Ed.; Springer International Publishing: Cham, Switzerland, 2019; pp. 387–414, ISBN 978-3-319-93169-2.
19. Ng-Cutipa, W.L.; González, F.J.; Lobato, A.; Zananiri, I.; Teodoro, A.C. Titanium, Zirconium and Rare Earth Element Placer Deposits in Coastal Environments of Rías Baixas (Galicia, NW Spain). In Proceedings of the Underwater Minerals Conference, Rotterdam, The Netherlands, 1–6 October 2023; p. 4. [CrossRef]
20. Ng-Cutipa, W.L.; Lobato, A.; González, F.J.; Zananiri, I.; Georgalas, G.; Teodoro, A.C.; Støren, J.; Myrnes, I.; S34i Shallow Water Team. Marine Placer Occurrences and Associated Critical Raw Materials in Rias Baixas (NW Spain). In Proceedings of the 37th International Geological Congress 2024, Busan, Republic of Korea, 25–31 August 2024.
21. Ng-Cutipa, W.L.; Lobato, A.; González, F.J.; Georgalas, G.; Zananiri, I.; Cardoso-Fernandez, J.; Carvalho, M.; Azzalini, A.; Araújo, B.L.; Teodoro, A.C. Earth Observation Approach to Understand Coastal Morphology, Shoreline Dynamics, and Their Relationship with Mineral Placer Deposits: The Case of Santa Marta Beach (Ría de Vigo, NW Spain). In Proceedings of the Abstracts Volume IX International Symposium on Marine Sciences (ISMS24), Valencia, Spain, 10–12 July 2024.

22. Carvalho, M.; Cardoso-Fernandes, J.; González, F.J.; Teodoro, A.C. Comparative Performance of Sentinel-2 and Landsat-9 Data for Raw Materials' Exploration Onshore and in Coastal Areas. *Remote Sens.* **2025**, *17*, 305. [CrossRef]
23. Cardoso-Fernandes, J.; Silva, J.; Dias, F.; Lima, A.; Teodoro, A.C.; Barrès, O.; Cauzid, J.; Perrotta, M.; Roda-Robles, E.; Ribeiro, M.A. Tools for Remote Exploration: A Lithium (Li) Dedicated Spectral Library of the Fregeneda–Almendra Aplite–Pegmatite Field. *Data* **2021**, *6*, 33. [CrossRef]
24. Carvalho, M.; Cardoso-Fernandes, J.; Lima, A.; Teodoro, A.C. Convolutional Neural Networks Applied to Antimony Quantification via Soil Laboratory Reflectance Spectroscopy in Northern Portugal: Opportunities and Challenges. *Remote Sens.* **2024**, *16*, 1964. [CrossRef]
25. McFeeters, S.K. The Use of the Normalized Difference Water Index (NDWI) in the Delineation of Open Water Features. *Int. J. Remote Sens.* **1996**, *17*, 1425–1432. [CrossRef]
26. Kruse, F.A.; Lefkoff, A.B.; Boardman, J.W.; Heidebrecht, K.B.; Shapiro, A.T.; Barloon, P.J.; Goetz, A.F.H. The Spectral Image Processing System (SIPS)—Interactive Visualization and Analysis of Imaging Spectrometer Data. *Remote Sens. Environ.* **1993**, *44*, 145–163. [CrossRef]
27. Clark, R.N. Spectroscopy of Rocks and Minerals and Principles of Spectroscopy. In *Manual of Remote Sensing, Volume 3, Remote Sensing for the Earth Sciences*; Rencz, A.N., Ed.; Wiley: Hoboken, NJ, USA, 1999; pp. 3–58.
28. Hunt, G.R. Visible and Near-Infrared Spectra of Minerals and Rocks: III. Oxides and Hydro-Oxides. *Mod. Geol.* **1971**, *2*, 195–205.
29. Hunt, G.R.; Salisbury, J.W.; Lenhoff, C.J. Visible and near Infrared Spectra of Minerals and Rocks. VI. Additional Silicates. *Mod. Geol.* **1973**, *4*, 85–106.
30. Divya, Y.; Sanjeevi, S.; Ilamparuthi, K. A Study on the Hyperspectral Signatures of Sandy Soils with Varying Texture and Water Content. *Arab. J. Geosci.* **2014**, *7*, 3537–3545. [CrossRef]